PHYSICS DESIGN OF FRONT ENDS FOR SUPERCONDUCTING ION LINACS*

P.N. Ostroumov†, ANL, Argonne, IL 60439 USA
J.-P. Carneiro‡, FNAL, Batavia, IL 60510, U.S.A.

Abstract

Superconducting (SC) technology is the only option for CW linacs and is also an attractive option for pulsed linacs. SC cavities are routinely used for proton and H^- beam acceleration above 185 MeV. Successful development of SC cavities covering the lower velocity range (down to 0.03c) is a very strong basis for the application of SC structures in the front ends of high energy linacs. Lattice design and related high-intensity beam physics issues in a ~400 MeV linac that uses SC cavities will be presented in this talk. In particular, axially-symmetric focusing by SC solenoids provides strong control of beam space charge and a compact focusing lattice. As an example, we discuss the SC front end of the H^- linac for the FNAL Proton Driver.

INTRODUCTION

High-intensity proton accelerators based on superconducting (SC) linacs have experienced a spectacular development over the last decade [1]. These proton drivers can deliver up to multi-MW beams in either CW or pulsed mode (<100 Hz) and are being developed for applications such as spallation neutron sources, production of radioactive ion beams (RIB), transmutation of nuclear waste or neutrino physics. Typical kinetic energies for such linacs range from 40 MeV to 8 GeV.

Due to the RF power consumption, high duty factor or CW operation of high power accelerators is inconceivable with Normal Conducting (NC) cavities and SC technology becomes the natural choice. Examples for CW ion drivers based on SC linacs are the heavy-ion linac ATLAS operated at ANL [2] or the multi-user facility SARAF [3] being constructed in Israel which is expected to deliver in 2010 deuteron beams with an energy of 40 MeV at 80 kW beam power. The proposed RIB facilities AEBL [4] and EURISOL [5] aim at delivering ion beams at an energy of respectively >200 MeV/u and 1 GeV for a corresponding beam power of 400 kW and 5 MW.

The development of SC cavities for $\beta<1$ gave rise in the recent years to several SC pulsed proton drivers. The Spallation Neutron Source accelerator (SNS, [6]) at Oak Ridge is, as of today, the only pulsed SC proton driver in operation. Its final goal is to deliver a proton beam of 1.0 GeV and 1.4 MW at a repetition rate of 60 Hz for neutron scattering research. Several other pulsed SC proton drivers are under development for neutron production like the Japan Proton Accelerator Research Complex linac [7] (J-PARC, 1.3 GeV, 10 MW, 50 Hz) or for neutrino physics like the CERN Superconducting Proton Linac [8] (SPL, 5 GeV, 4 MW, 50 Hz) or the Fermilab Proton Driver [9] (FNAL PD, 8 GeV, 2 MW, 10 Hz). The main mission of the FNAL PD is to increase the intensity of the Main Injector. This paper describes the physics design of the FNAL PD SC front-end (~420 MeV). A detailed description of the full linac is presented in [10].

FRONT END DESIGN

The main concern in the design of the FNAL PD (as for any high-intensity proton linac) is the control of the beam losses at a level that allows ”hands-on maintenance”. Experience on the LANSCE accelerator at Los Alamos has lead the accelerator community to take as a rule of thumb that ”hands-on maintenance” is possible if uncontrolled losses along the linac are kept below 1 W/m. For the FNAL PD operating at 2 MW, this means a relative loss of only $5\cdot10^{-7}$ particle per meter. As a consequence, particular attention has been taken in the design of the front-end of the linac to control the growth of beam halo that would lead to particle losses.

Why Spoke Resonator?

Typical front-end designs for proton drivers are made of NC structures (like Drift Tube Linac and Coupled Cavity Linac) with a transition to SC ones at high energy: 160 MeV for the SPL, 185 MeV for SNS or 400 MeV for J-PARC. An original approach has been taken for the design of the front-end of the FNAL PD. Taking advantage of the development and excellent performance of spoke cavities [11,12] it was decided to make a transition from NC to SC structures at low energy. From ~10 MeV to ~420 MeV the beam will be accelerated with SC Single Spoke Resonators and SC Triple Spoke Resonators. Compared to standard NC accelerating structures, the SC cavities offer higher accelerating gradients and cost-effective operation. Furthermore, the use of high-power ferrite vector modulators [13] allows the fan-out of RF power from a klystron to feed multiple cavities. With this outstanding feature of the FNAL PD, only five J-PARC type 2.5 MW klystrons are necessary to power the 420-MeV front-end of the linac while, for instance, the SNS 186-MeV front-end requires 11 klystrons.

Why Superconducting Solenoid ?

SC solenoids have been selected as the focusing elements for the front-end (up to ~120 MeV limited by H^-

* Work supported by the U.S. Department of Energy, under Contracts No. DE-AC-02-06CH11357 and DE-AC02-07CH11359.
† ostroumov@anl.gov
‡ carneiro@fnal.gov

Figure 1: Schematic layout of the front-end of the FNAL 8-GeV superconducting linac.

Table 1: Main parameters for each section of the front-end linac with focusing type (S: Solenoid, R: Resonator, nR: n Resonators, F: Focusing quad. and D: Defocusing quad).

Section No.	Section Name	Wout (MeV)	Cavities No.	Focusing Type	Period No.	Lf (m)	z (m)
1	CH	10	16	S1R	16	0.49-0.75	17
2	SSR1	32	18	S1R	18	0.75	31.4
3	SSR2	124	33	S2R	18	1.6	61.0
4	TSR	421	42	FRDR	21	3.8	142.2
Total		~421	109		73		~142.2

stripping) of the FNAL PD in lieu of the standard quadrupole structures.

The idea of using SC solenoids in the front-end of high-intensity SC proton linacs was discussed conceptually by Garnett [14]. Our design differs from [14] by efficient use of the available voltage from SC cavities and provides much higher real-estate gradients tighter with better control of space charge by reduced length of the focusing periods.

Several advantages arise from the use of SC solenoids:

- to provide stability for all particles inside the separatrix the defocusing factor

$$\gamma_s = \frac{\pi}{2}\frac{1}{(\beta\gamma)^3}\frac{L_f^2}{\lambda}\frac{eE_m \sin(\varphi_s)}{m_0 c^2} \quad (1)$$

  should be kept below ~0.7. SC solenoids shorten the length of the focusing period (by a factor of 2 compared to FODO focusing) which facilitates the use of the higher accelerating gradients offered by the SC cavities. In Eq. 1 : m_0c^2 is the particle rest energy, β is the particle relative velocity, γ is the Lorentz factor, λ is the wavelength of the RF field, L_f is the length of the focusing period, E_m is the amplitude of the equivalent traveling wave of the accelerating field and φ_s is the synchronous phase
- the smooth axial-symmetric focusing provided by SC solenoids in the MEBT mitigates the formation of halo which can take place with weak asymmetric focusing as observed at SNS [15]
- as discussed in [16], lattices using SC solenoids are less sensitive to misalignments, errors and beam mismatches.

Furthermore, SC solenoids are perfectly suitable for SC environment with SRF. SC solenoids are easily re-tunable to adjust to the accelerating gradient variation from cavity to cavity and can they can also be supplemented with dipole coils for corrective steering of the beam centroid. SC solenoids have been used at ATLAS facility for several decades [2] and implemented in new facilities such as ISAC-II [17] and SARAF [3].

FNAL Proton Driver front-end lattice

A schematic layout of the front-end of the FNAL PD is presented in Figure 1. The different sections of the linac with corresponding main parameters are presented in Table 1. The linac front-end is made of 73 focusing periods with lengths varying from 49 cm to 3.8 m. The H^- beam from the Ion Source is bunched and accelerated up to 2.5 MeV by a 325 MHz RFQ. At that energy the MEBT section provides space for a fast beam chopper (<2 ns) to eliminate unwanted bunches and forms an optimal beam time structure for injection into the Main Injector. This chopping decreases the beam average current over the 1 msec pulse from ~45 mA to ~25 mA. Acceleration from 2.5 MeV to 10 MeV is provided by 16 room temperature cross-bar H-type (CH) cavities. The CH cavities, foreseen for the future proton synchrotron of GSI [18], present very high shunt impedance (90 MOhm/m to 60 MOhm/m) and are an excellent option. The use of SC technology is not appropriate for this energy range as it would require time-consuming and expensive development of multiple SC designs. Above 10 MeV, SC RF structures are used. Two types of Single Spoke Resonators and one type of Triple Spoke Resonator (SSR1, SSR2 and TSR) accelerate the beam up to ~420 MeV. At this energy, spoke cavities become less

efficient and the beam is further accelerated up to 8 GeV using Squeezed ILC (β_g=0.81) and ILC (β_g=1) 1.3 GHz cavities. The frequency transition at 420 MeV is favorable to longitudinal beam dynamics [10].

FRONT END SIMULATIONS

The main tool used for the design of the FNAL PD is the beam dynamics code TRACK [19]. For benchmarking purposes, the simulations have also been performed with the code ASTRA [20] developed by DESY. Mainly used for the design of electron photo-injectors, it offers also the possibility of simulating hydrogen ion beams. Both codes handle 3D space charge. Benchmarking starts at the RFQ exit since ASTRA does not cover RFQ beam dynamics.

The Radio Frequency Quadrupole

The FNAL RFQ is ~3 m long and is capable of efficiently accelerating bunch beam currents up to 140 mA. The RFQ physics design and beam dynamics simulations were presented elsewhere [21]. One original point in the design of the RFQ is the use of an output radial matcher to produce axially-symmetric beam. Particular attention was taken to preserve transverse emittance and to minimize the longitudinal emittance while maximizing the accelerating rate.

Front-end beam dynamics

The design of the FNAL PD has been performed following the general design requirements for high-intensity proton linacs [10] necessary to minimize RMS emittance growth along the linac:

- keep the zero current phase advance per focusing period in all planes below 90° to avoid parametrically-excited instabilities at high current
- provide smooth evolution of the wavenumbers ($k_{T0,}$ and k_{L0}) of both transverse and longitudinal oscillations along the linac. This feature minimizes the potential for mismatch and helps assure a current independent lattice. The wavenumbers of particle oscillations are expressed as $k_{T0} = \frac{\sigma_{T0}}{L_f}, k_{L0} = \frac{\sigma_{L0}}{L_f}$, where σ_{T0}, σ_{L0} are the transverse and longitudinal phase advance per focusing period of length L_f at zero current
- avoid the n=1 parametric resonance between the transverse and longitudinal motion. The condition for occurrence of an n-th order parametric resonance of transverse motion to occur is $\sigma_{T0} = \frac{n}{2}\sigma_{L0}$. The strongest resonance is for n=1 and can occur particularly in SC linacs due to the availability of high accelerating gradients and relatively long focusing periods. It can be avoided by properly choosing the linac operation tunes in the Kapchinskiy stability diagram
- avoid strong space-charge resonances by selecting stable areas in the Hofmann's stability charts or use fast resonance crossing
- maintain beam equipartitioning to avoid energy exchange between the transverse and longitudinal planes that can occur via space-charge forces

For NC linacs all the above listed requirements can be fulfilled with peak currents up to ~150 mA as presented in reference [22]. Cost-effective SC linacs are more challenging for satisfying these specifications. For example, cavities and focusing elements in SC linacs are located in relatively long cryostats with inevitable drift spaces between them. Also, the focusing period lengths can present a sharp change at transitions between linac sections with different types of cavities.

Figure 2 presents TRACK and ASTRA simulations of the FNAL PD font-end linac at zero current. The variation of the transverse and longitudinal phase advance along the linac is presented in Fig. 2(a). The observable, but insignificant, difference between the phase advances from TRACK and ASTRA comes primarily from the different technique of calculation of the phase advances. Due to the changing length of the focusing period at transitions between different types of SC cavities, the phase advances present strong but innocuous jumps. Apart from few periods, the phase advances remain below 90°. Figure 2(b) shows the smooth change of the transverse and longitudinal wavenumbers along the linac. The smooth evolution of the transverse wavenumber is provided by selecting the appropriate length of the focusing periods (as shown in Table 1) and focusing field strengths. Concerning the longitudinal wavenumber, smooth evolution is obtained by properly adjusting the synchronous phase of each cavity. The Kapchinskiy stability diagram [Fig. 2(c)] presents the evolution of $\cos(\sigma_{0T})$ as a function of the defocusing factor γ_s (Eq. 1). The gray area corresponds to the n=1 parametric resonance and the dashed line corresponds to the stability required for the particles near the separatrix boundary at a phase angle of $-2|\varphi_s|$. The majority of the 73 period tune points are located in the stable areas of the Kapchinskiy diagram. The few tune points located outside the stability region correspond to the first focusing periods of the CH section. These regions present essentially no problem since the instability takes place over a short distance compared to the betatron oscillation wavelengths.

Figure 3 presents the Hofmann's stability chart [23] for the FNAL PD front-end at the design current of 45 mA for a longitudinal to transverse emittance ratio of $\varepsilon_L/\varepsilon_T$=2. The shaded areas indicate regions where nonequipartitioned beams are subject to space charge coupling resonances that are expected to cause emittance transfer. The dangerous resonance in the chart is the 4-th

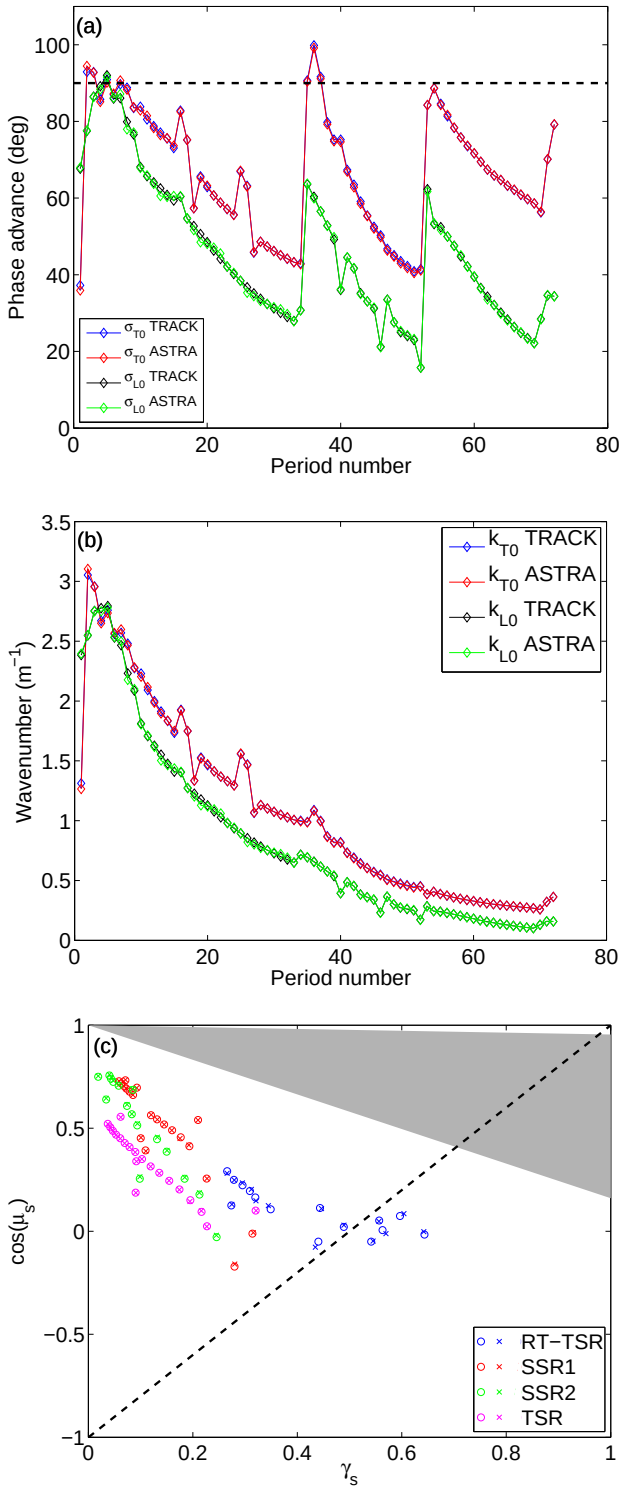

Figure 2: TRACK and ASTRA simulations of the FNAL PD front-end at zero current : (a) trans. and long. phase advances, (b) trans. and long. wavenumbers and (c) Kapchinkiy stability diagram. The gray area in (c) shows the boundary of the n=1 parametric resonance and the dashed line particle located near the separatrix. In (c) circles represent TRACK and crosses ASTRA.

order even mode one located around a tune ratio of 1. The peaks on the left represent weak coupling resonances that would take a long time to develop. As depicted in Fig. 3, TRACK and ASTRA predict a moderate tune depression (between 0.5 and 0.8) with most of the operating tunes lying in stable (white) areas. Therefore space charge driven resonances are not a concern for the current design of the FNAL PD front-end.

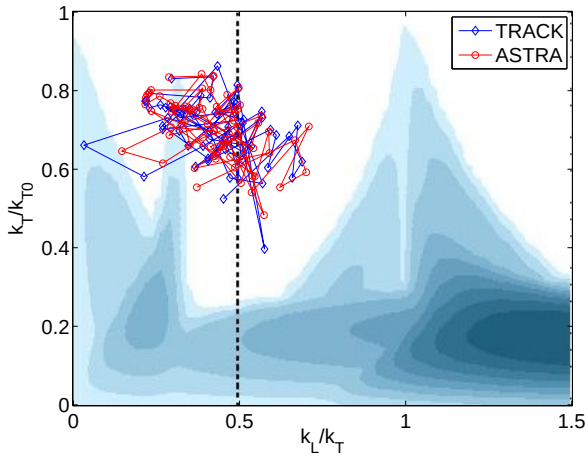

Figure 3: Hofmann's chart for a long. to trans. emittance ratio of 2. See text for details. Courtesy of I. Hofmann.

Emittance growth and beam losses

Figure 4 shows simulated transverse and longitudinal emittance growth for the FNAL PD front-end which is at an acceptable level and is mainly due to imperfection matching at the lattice transitions. A detailed beam loss analysis of the full linac reported in [24] using TRACK shows that the actual design indicates very limited losses for typical misalignments and RF errors. The use of SC cavities with large apertures enables the ratio aperture-to-RMS-beam-size to stay higher than 10 in most of the linac which helps avoid losses.

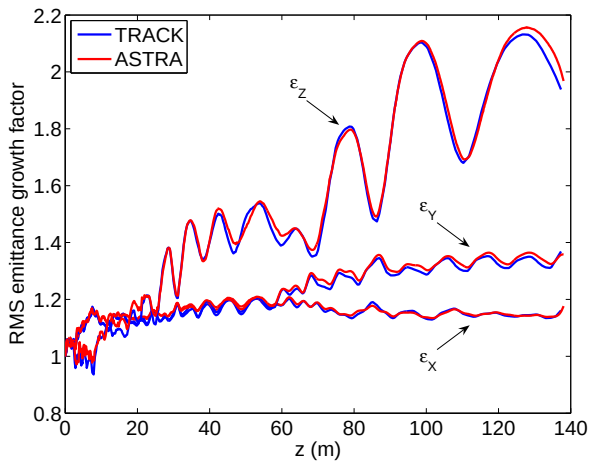

Figure 4: RMS trans. and long. emittance growth factor in the FNAL PD front-end at 45mA. From TRACK and ASTRA with $2 \cdot 10^5$ macro-particles.

Front-end at 100 mA

The front-end design developed for the FNAL PD can be successfully applied for acceleration of 100 mA proton/H^- beams. As was shown by LANL during the work on several projects, for high-intensity beams above ~100 mA it is reasonable to use an RFQ up to ~7 MeV. Below we discuss a front-end based on the FNAL PD lattice but with 7 MeV RFQ. For the purpose of beam dynamics simulations we assume that perfect 6D matching is provided at the entrance of the linac at 7 MeV. The lattice beyond 7 MeV is the same as in FNAL PD linac with slightly different geometrical beta of SSR1 and SSR2 for better matching to beam velocity. As shown in Figure 5 good beam matching is provided in the transitions resulting in a very low emittance growth factor of the 100 mA beam. Even the 99.5 % total emittance depicted in Fig. 5(b) presents a moderate growth factor indicating a limited halo formation.

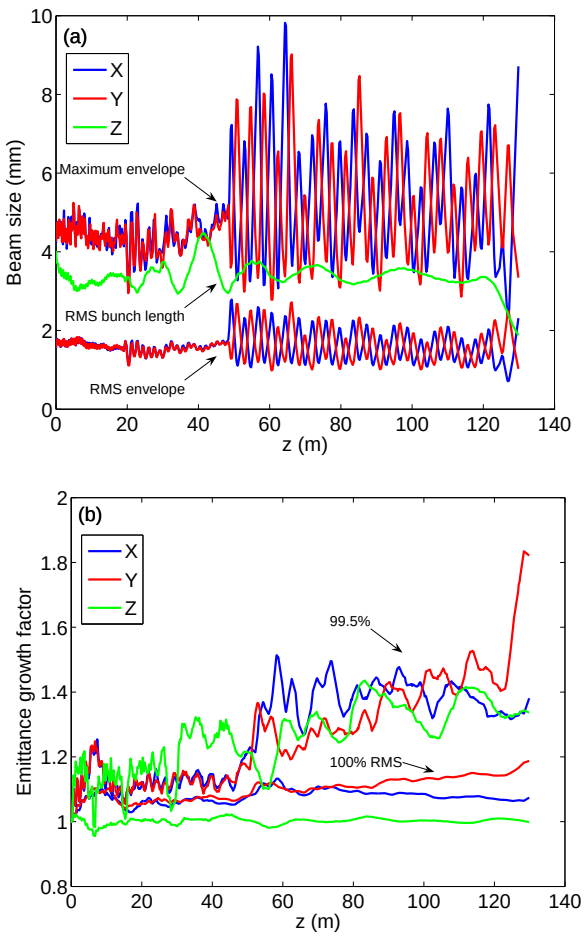

Figure 5: Front-end from 7 MeV to 420 MeV at 100 mA: (a) beam envelopes and (b) 100% RMS and 99.5% total emittance growth factor. From TRACK.

CONCLUSION

A SC front-end presents a competitive option for high-intensity ion linacs, not only in terms of power consumption but also to ensure high-quality beams. The front-end of the FNAL PD accelerates beams from the Ion Source up to 420 MeV using CH cavities to ~10 MeV followed by SC spoke (SSRs and TSRs) resonators. All operate at the 4th sub-harmonic of the ILC frequency. The use of SC solenoids results in a compact lattice below ~120 MeV and facilitates the use of the high accelerating gradients offered by the SSR cavities. Also SC solenoids help mitigate halo formation and beam losses.

REFERENCES

[1] F. Gerigk, CERN-AB-2007-035
[2] R. Pardo, “Long-Term Operating Experience for the Atlas Superconducting Resonators”, SRF99.
[3] C. Piel et al., “Phase 1 commissioning of the 40 MeV Proton/Deuteron Accelerator SARAF’, EPAC08.
[4] B. Mustapha et al. “A driver linac for the advanced exotic beam laboratory (…)”, PAC07.
[5] J.-L. Biarrotte, “High power CW superconducting linacs for EURISOL and XADS”, LINAC04.
[6] A. Aleksandrov et al., “Performance of the SNS front end and warm linac”, EPAC08.
[7] K. Hasegawa, “Commissioning of the J-PARC Linac”, PAC07.
[8] F. Gerigk (ed.), CERN-2006-006.
[9] G.W. Foster (ed.), available at: http://protondriver.fnal.gov/#Technical_Design_Link .
[10] P.N. Ostroumov, New J. of Physics, 8, 281, 2006.
[11] M.P. Kelly, “Overview of TEM-Class Superconducting Cavities for Proton and Ion Acceleration”, LINAC 2006
[12] K. W. Shepard, P. N. Ostroumov, and J. R. Delayen, Phys. Rev. ST – AB 6, 080101, 2003.
[13] R. Madrak et al., “New Materials and Designs for High-Power Fast Phase Shifters”, LINAC06.
[14] R. W. Garnett et al., “Conceptual Design of a Low-β SC Proton Linac”, PAC01
[15] D. Jeon, “Beam Dynamics in the Spallation Neutron Source”, PAC03.
[16] B.I. Bondarev et al., translated from Atomnay Energiya, Vol. 34, No. 2, pp. 131-133, Feb. 1973.
[17] M. Marchetto et al, “Beam dynamics studies of the ISACII Superconduting Linac”, LINAC06.
[18] Z. Li, “Design of the RT CH-Cavity and Perspectives for a new GSI Proton Linac”, LINAC04.
[19] V.N. Aseev et al. “TRACK : The new beam dynamics code”, PAC05.
[20] K. Floettmann, ASTRA user manual available at: http://www.desy.de/~mpyflo/Astra_dokumentation/
[21] P.N. Ostroumov et al., J. of Inst., P04002, 2006.
[22] G.P. Lawrence and T.P. Wangler, “Integrated Normal-Conducting/Superconducting High Power Proton Linac for APT Project”, PAC97.
[23] I. Hofmann, Phys. Rev. E 57, 4713, 1998.
[24] P.N. Ostroumov et al., “Beam dynamics studies of the 8-GeV superconduting H^- linac”, LINAC06.